

in vivo Sodium Imaging at 4T using Conical-SPRITE and 3D GRE: a First Comparison

S. Romanzetti¹, J. Kaffanke¹, M. Halse², B. Balcom³, N. J. Shah^{1,4}

¹Institute of Medicine, Research Centre Juelich, Juelich, Germany, ²University of New Brunswick, Fredericton, New Brunswick, Canada, ³Department of Physics, University of New Brunswick, Fredericton, New Brunswick, Canada, ⁴Institute of Physics, University of Dortmund, Dortmund, Germany

Introduction

The vast majority of physiological processes taking place in the cell rely upon highly regulated intra- (10 mM) and extracellular (150 mM) sodium ion concentrations. The main mechanism at the basis of this fine regulation is the Na/K pump. Variations of sodium concentration from these values are indicative of diseases that imply metabolic changes and that might alter the normal function of the Na/K pump itself. The measurement of Tissue Sodium Concentration (TSC) [1] is therefore important to understand disease grade and tissue viability. However, difficulties such as low sensitivity and complex relaxation behaviour are associated with ²³Na imaging. In tissues, the quadrupole moment of the ²³Na nucleus ($I = 3/2$) determines a complex transverse relaxation mechanism of the outer transitions ($3/2 \leftrightarrow 1/2$ and $-3/2 \leftrightarrow -1/2$) that causes the signal to decay according to a biexponential law with a fast component on the order of a few milliseconds. Thus, ²³Na imaging requires special imaging strategies. In this study, *in vivo* ²³Na images acquired using Conical-SPRITE are compared to images acquired using an optimised 3D Gradient Echo on a normal healthy volunteer brain. Conical SPRITE images show very good signal-to-noise ratios but are characterised by blurring which hinders exact anatomical determination. On the other hand, 3D GRE delivers images with good anatomical details but almost completely loses the fast component of the ²³Na signal.

Methods

All experiments were performed on a whole-body 4T Unity Inova scanner (Varian, Palo Alto, CA) with a maximum gradient of 40 mT/m and 200 mT/m/ms slew rate. The RF probe was a home-built 4 rung birdcage coil.

Conical SPRITE

Figure 1 depicts the timing diagram of the multiple point Conical-SPRITE sequence. A short non-selective RF excitation pulse is applied in the presence of 3D phase encoding gradients and after an encoding time $t_p \ll T_2^*$, a series of m FID points at equally spaced time intervals, Δt_p , are acquired. Each last point of the series falls on the Cartesian grid. The excitation-detection scheme is repeated for each net gradient step of the waveforms describing cones in the k-space. Finally, the acquired multiple FID points were used to reconstruct independent k-spaces of slightly different fields-of-view (FOV). To re-zoom the images to a common field-of-view, the chirp-z transform algorithm was employed [2], allowing for final signal averaging. Conical SPRITE images were acquired using the following parameters: FOV=240×240×240mm, matrix size = 32×32×32 (voxel volume of 421.87mm³), $t_p=0.5$ ms, TR=1.0ms, flip=3°, sw=29kHz, $m=9$, $\Delta t_p=31.25\mu$ s, NEX=150, total acquisition time=31 min.

3D Gradient Echo

3D ²³Na images were acquired using a 3D Gradient echo sequence which was optimized to maximize SNR [3]. The acquisition parameters were as follows: FOV=240×240×240, matrix size = 64×64×24 (voxel volume=140.625mm³), 25% asymmetric echo, TE=3.4ms, tr=20.0ms, sw=6.4kHz, flip= 40°, NEX=32, total acquisition time=21 min 36 sec.

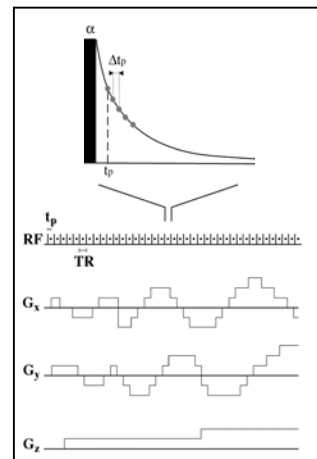


Fig.1 timing diagram of multiple point Conical-SPRITE

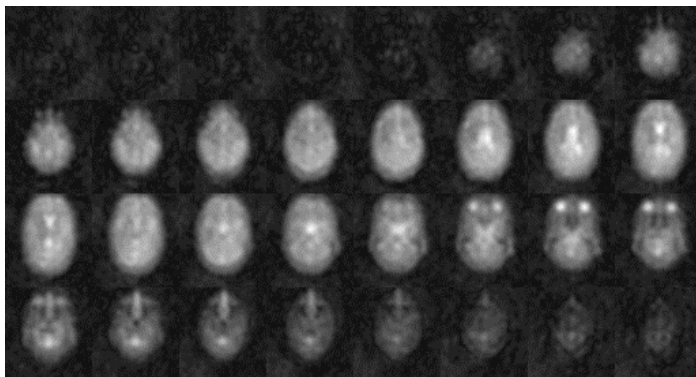


Fig. 2 Conical SPRITE images, Transaxial section

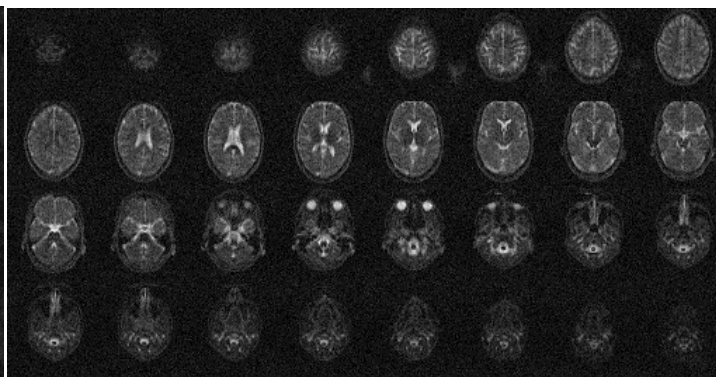


Fig. 3 3D GRE images, Transaxial section

Results

Figure 2 shows *in vivo* ²³Na images of a healthy human brain obtained using Conical-SPRITE. Nine multiple FID points with a dwell time of $\Delta t_p=31.25\mu$ s were acquired after each excitation pulse. By virtue of the multiple-point acquisition, the images in Fig 2 are equivalent to $150 \times 9 = 1350$ normal averages. The power deposition was monitored during the whole acquisition and was less than the local limit of 8 W/kg over the entire acquisition time. The SNR (scaled by voxel volume ratio, $r=3$) calculated in the CSF, brain tissue (including grey and white matter) and the eyes was $34/(3 \times 3)$, $24/(3 \times 3)$ and $29/(3 \times 3)$, respectively. For noise determination, the standard deviation of a background region-of-interest was employed.

Figure 3 shows *in vivo* ²³Na images of the same brain obtained using 3D GRE. High in-plane resolution allows for accurate detection of anatomical structures. The SNR calculated in the same areas as for Conical SPRITE, i.e. CSF, brain tissue and the eyes was 32, 10, 28, respectively. To determine noise, the standard deviation of a background region-of-interest was employed. A comparison of the intra-method SNR ratios between brain tissues and CSF for both imaging modalities ($24/34$ for Conical-SPRITE and $10/32$ for 3D GRE) denotes the ability of Conical-SPRITE to sample the sodium signal during its biexponential regime (in this case after $t_p=500\mu$ s). The 3D GRE signal, on the other hand, is mainly weighted by long T_2^* components given the longer echo time (TE=3.4 ms).

Discussion

The Conical-SPRITE sequence combines the advantages of Single Point Images pulse sequences for visualising and quantifying fast decaying nuclei with a very fast and flexible k-space sampling scheme which allows one to obtain images of the total sodium concentration in the brain in a very simple way. However, the low-resolution images obtained might be better interpreted by an overlay with a high-resolution ¹H anatomical image. Conventional sequences tend to underestimate the sodium signal because the fast-decaying component is neglected but still provide higher anatomical details. In conclusion, Conical SPRITE with optimised acquisition offers a fast, and reliable way to image the sodium concentration in the brain, which will prove critical for the diagnosis and the monitoring of pathologies leading to sodium concentrations changes in the brain.

References: [1] K. Thulborn *et al.*, Radiology 213:156(1999), [2]. M. Halse *et al.*, JMR 169:102(2004), [3]. T. Parrish *et al.*, MRM 38:653(1997).